Supplementary for Learning Active Force-torque based Policy for Sub-mm Localization of Unseen Holes

Liang Xie[✉], **Haodong Zhang, Yinghao Zhao, Yue Wang**[✉], **Rong Xiong**[✉]

State Key Laboratory of Industrial Control Technology
and Institute of Cyber-Systems and Control,
Zhejiang University, Zhejiang, China

1. Introduction

In this document, we provide the details mentioned in the main paper, including the description of the hybrid position-force controller, the control mode, and the performance on different peg and hole materials.

A. Hybrid Position-force Controller

We use the hybrid position-force controller to track the 3-DoF end-effector motions (see Fig. 1). We define the world frame as $\{R\}$ by taking the robot base as the origin in the coordinate system. We also define the reference frame as $\{P\}$, which is attached to the robot end-effector. For the position control, the desired 2D action $\mathbf{a}_\mathrm{t} = [dx, dy]$ produced by the policy is executed by a PD controller with the control law defined as:

$$\mathbf{e}_\mathrm{q} = \mathbf{S}\mathbf{J}^{-1}(\mathbf{a}_\mathrm{t} - \mathbf{T}_R^P\mathbf{J}\mathbf{q}) \tag{1}$$

$$\mathbf{u}_\mathrm{m} = k_{pm}\mathbf{e}_\mathrm{q} + k_{vm}\dot{\mathbf{e}}_\mathrm{q} \tag{2}$$

where $\mathbf{S}$ is the diagonal matrix to decouple the position and the force control, $\mathbf{J}$ is end-effector Jacobian, $\mathbf{T}$ is the transform matrix from $\{R\}$ to $\{P\}$, $\mathbf{q}$ is joint displacement in joint space, k_{pm} and k_{vm} are proportional gain and differential gain, respectively. The PD controller takes the desired end-effector position from the policy at 300 Hz and outputs the robot command at 1000 Hz. On the z-axis, we use force control to locate the hole surface and maintain the constant contact force $\mathbf{f}_\mathrm{d}$ between the peg and the hole by a PI controller. The control law is defined as:

$$\mathbf{e}_\mathrm{f} = -\mathbf{S}(\mathbf{f}_\mathrm{d} - \mathbf{f}_\mathrm{t}) \tag{3}$$

$$\mathbf{u}_\mathrm{f} = \mathbf{J}^\mathrm{T}(k_{pf}\mathbf{e}_\mathrm{f} + k_{if}\int \mathbf{e}_\mathrm{f} - \mathbf{S}\mathbf{f}_\mathrm{d}) \tag{4}$$

where $\mathbf{f}_\mathrm{t}$ is the force feedback from the F/T sensor, k_{pf} and k_{if} are the proportional gain and the integral gain respectively. The force-torque sensor communicates with the computer via a TCP socket at 100 Hz. Tab.1 summarizes the coefficients of the controller.

Table 1. Controller Coefficients

Coefficient	Value
PD proportional gain (k_{pm})	20
PD differential gain (k_{vm})	5
PI proportional gain (k_{pf})	0.004
PI integral gain (k_{if})	1
Constant contact force ($\mathbf{f}_\mathrm{d}$)	10N

B. Control Mode

We choose the discrete position control instead of the continuous speed control because the measured forces and torques include the friction forces and torques, which are produced in the sliding between the peg-hole surfaces. In continuous control, the peg could slide in different directions and cause different friction forces and torques. Hence, the measured forces and torques will differ from the static ones in the pre-collected dense map, leading to failure in the following localization and matching. To solve the problem, we control the peg above the hole surface without contact at each time step of the position control. The robot starts by receiving the actions produced

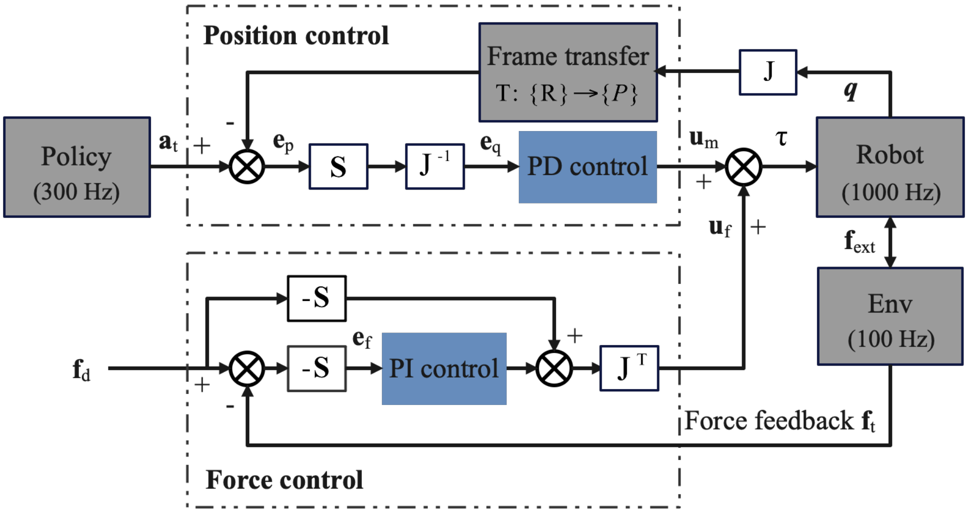

Fig. 1. The hybrid position-force controller.

by the policy and outputting the torque commands to move the peg to the desired position. Then the contact forces and torques are measured and recorded as the observation of the next time-step. Finally, a small upwards move is initiated to keep the peg apart from the hole surface and prepare for the next control cycle. The videos of the experiments are available at `https://github.com/xieliang555/Tracer` for a more intuitive understanding. We use this control mode to minimize the uncertainty introduced by the friction forces and torques. Although the insertion efficiency and fluency decline to a certain extent by adopting this control mode, we find promising results in the generalization potential to unseen peg-hole pairs in the real world.

C. *Performance on Different Materials*

In the main manuscript, we have conducted experiments with the 3D-printed peg-hole models and various tight connector-socket pairs (e.g., USB, Type-C, C13, RJ-45). The materials of those pairs are very different. For example, the USB and Type-C mating parts are made of rigid metal. The RJ-45 (PC plastic) and the 3D-printed models (ABS plastic) are made of plastic materials with higher elasticity. Based on preliminary experiments, we further conduct experiments with a rubber connector made up of slightly deformable materials. We combine the peg-hole pairs with different materials, such as metal peg+metal hole (USB, Type-C), PC plastic peg+metal hole (RJ-45), ABS plastic peg+ABS plastic hole (3D-printed models), and rubber peg+metal hole (3-pin electric plug) as shown in Fig.2. The experiment results are summarized in Tab.2. We can find that our method can generalize to peg-hole pairs with different materials and elasticity. The experiment videos are available at `https://github.com/xieliang555/Tracer`

Table 2. *Policy Success Rate on Different Peg-hole Materials*

Success Rate	**Peg-hole Material**			
	metal peg +metal hole	plastic(pc) peg +metal hole	plastic(abs) peg +plastic(abs) hole	rubber peg +metal hole
10-step	21/25	23/25	24/25	21/25
20-step	24/25	25/25	25/25	23/25

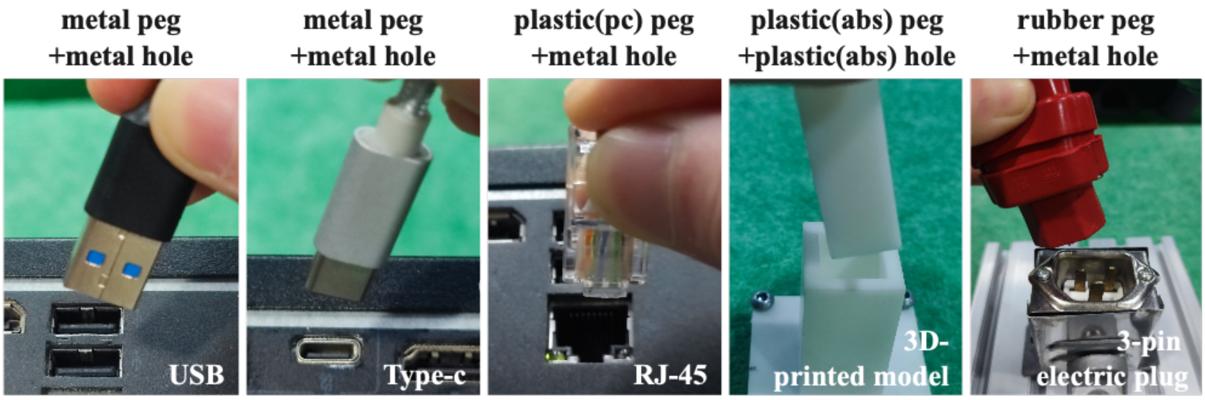

Fig. 2. The evaluated peg-hole pairs with different materials and elasticity.